Click Here for Full Article

Ice mélange dynamics and implications for terminus stability, Jakobshavn Isbræ, Greenland

J. M. Amundson,[1] M. Fahnestock,[2] M. Truffer,[1] J. Brown,[3] M. P. Lüthi,[3] and R. J. Motyka[1]

[1] We used time-lapse imagery, seismic and audio recordings, iceberg and glacier velocities, ocean wave measurements, and simple theoretical considerations to investigate the interactions between Jakobshavn Isbræ and its proglacial ice mélange. The mélange behaves as a weak, granular ice shelf whose rheology varies seasonally. Sea ice growth in winter stiffens the mélange matrix by binding iceberg clasts together, ultimately preventing the calving of full-glacier-thickness icebergs (the dominant style of calving) and enabling a several kilometer terminus advance. Each summer the mélange weakens and the terminus retreats. The mélange remains strong enough, however, to be largely unaffected by ocean currents (except during calving events) and to influence the timing and sequence of calving events. Furthermore, motion of the mélange is highly episodic: between calving events, including the entire winter, it is pushed down fjord by the advancing terminus (at $\sim$40 m d^{-1}), whereas during calving events it can move in excess of 50×10^3 m d^{-1} for more than 10 min. By influencing the timing of calving events, the mélange contributes to the glacier's several kilometer seasonal advance and retreat; the associated geometric changes of the terminus area affect glacier flow. Furthermore, a force balance analysis shows that large-scale calving is only possible from a terminus that is near floatation, especially in the presence of a resistive ice mélange. The net annual retreat of the glacier is therefore limited by its proximity to floatation, potentially providing a physical mechanism for a previously described near-floatation criterion for calving.

1. Introduction

[2] The recent thinning [Thomas et al., 2000; Abdalati et al., 2001; Krabill et al., 2004], acceleration [Joughin et al., 2004; Howat et al., 2005; Luckman et al., 2006; Rignot and Kanagaratnam, 2006], and retreat [Moon and Joughin, 2008; Csatho et al., 2008] of outlet glaciers around Greenland has stimulated a discussion of the processes controlling the stability of the Greenland Ice Sheet. These rapid changes are well correlated with changes in ocean temperatures both at depth [Holland et al., 2008] and at the surface [Howat et al., 2008]. Furthermore, velocity variations on these fast-flowing outlet glaciers appear to be linked to changes in glacier length and are largely unaffected by variations in surface melt rates [Joughin et al., 2008b]. Thus, the observed changes in glacier dynamics and iceberg calving rates are likely driven by processes acting at the glacier-ocean interface.

[3] Large calving retreats at some glaciers have been correlated with the loss of buttressing sea ice [e.g., Higgins, 1991; Reeh et al., 2001; Copland et al., 2007]. Likewise, the seasonal advance and retreat of Jakobshavn Isbræ (Figure 1) (Greenlandic name: Sermeq Kujalleq), one of Greenland's largest and fastest-flowing outlet glaciers, is well correlated with the growth and decay of sea ice in the proglacial fjord [Birnie and Williams, 1985; Sohn et al., 1998; Joughin et al., 2008c]. It therefore appears that sea ice, despite being relatively thin, may help to temporarily stabilize the termini of tidewater glaciers.

[4] Presently, calving ceases at Jakobshavn Isbræ in winter, causing the terminus to advance several kilometers and develop a short floating tongue [Joughin et al., 2008b; Amundson et al., 2008]. The newly formed tongue rapidly disintegrates in spring after the sea ice has retreated to within a few kilometers (or less) of the terminus [Joughin et al., 2008c] and before significant surface melting has occurred. The rapid disintegration of the newly formed tongue, which occurs over a period of a few weeks, suggests that the tongue is little more than an agglomeration of ice blocks that are prevented from calving by sea ice and ice mélange (a dense pack of calved icebergs). Note that we

[1]Geophysical Institute, University of Alaska Fairbanks, Fairbanks, Alaska, USA.
[2]Institute for the Study of the Earth, Oceans and Space, University of New Hampshire, Durham, New Hampshire, USA.
[3]Versuchsanstalt für Wasserbau, Hydrologie und Glaziologie, ETH Zurich, Zurich, Switzerland.
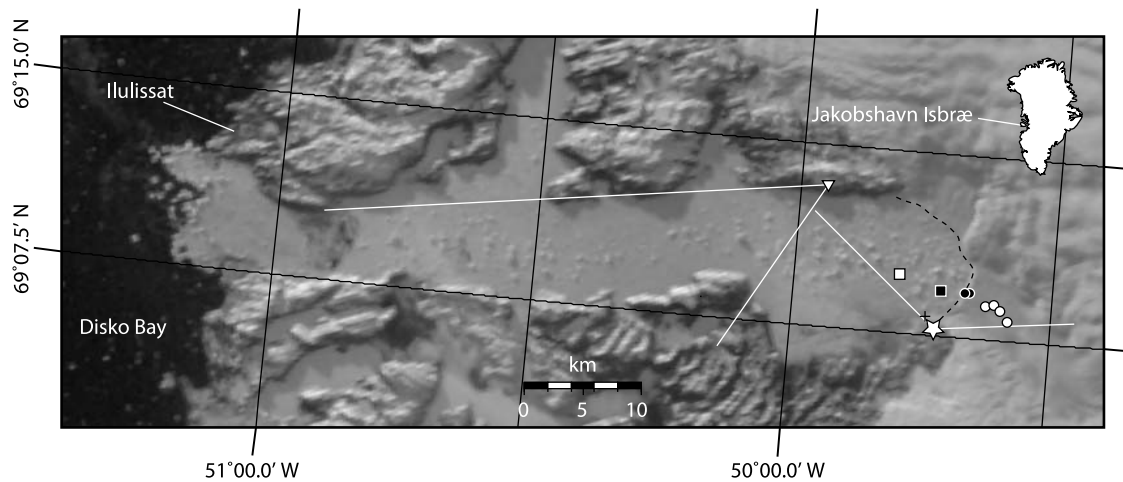
Figure 1. MODIS image of the terminal region of Jakobshavn Isbræ and proglacial fjord from 26 May 2007 (day of year 146). The terminus is marked with a dashed line. The seismometer, audio recorder, GPS base station, and one to six time-lapse cameras were located near our camp, indicated by a star. An additional camera was placed on the north side of the fjord (triangle) and pointed in the down fjord direction. The approximate field of view of the cameras is indicated by the white lines. Also indicated are the initial positions of the 2007 (black circles) and 2008 (white circles) surveying prisms used in Figure 3, the initial positions of the 2007 (black square) and 2008 (white square) iceberg GPS receivers, and the pressure sensor (small cross) that was used to measure ocean waves.

prefer the term ice mélange over the Greenlandic word "sikkusak" [e.g., *Joughin et al.*, 2008c], as observations presented here may be applicable to non-Greenlandic glaciers, such as to the Wilkins Ice Shelf during its recent disintegration [e.g., *Scambos et al.*, 2009; *Braun et al.*, 2009].

[5] Visual observations of Jakobshavn Isbræ's proglacial ice mélange suggest that (1) the mélange forms a semirigid, viscoelastic cap over the innermost $15-20$ km of the fjord, (2) motion of the mélange is primarily accommodated by deformation and/or slip in narrow shear bands within and along the margins of the mélange, and (3) icebergs within the mélange gradually disperse and become isolated from each other as they move down fjord. We propose that the mélange is essentially a weak, poorly sorted, granular ice shelf, and is therefore capable of influencing glacier behavior by exerting back pressure on the glacier terminus [*Thomas*, 1979; *Geirsdóttir et al.*, 2008]. When shear stresses within the mélange exceed some critical value, the mélange fails along discrete shear margins. Sea ice formation in winter stiffens the mélange matrix and promotes the binding of clasts (icebergs and larger brash ice components), thereby increasing the mélange's critical shear stress. Thus, sea ice and ice mélange may act together to influence glacier and terminus dynamics.

[6] Here, we use a suite of observations and simple theoretical considerations to investigate the dynamics of Jakobshavn Isbræ's ice mélange and possible mechanisms by which the mélange may influence glacier behavior. Our results have implications for fjord and glacier dynamics, the sequence and timing of calving events, and limitations on the glacier's rate of retreat.

2. Methods

[7] Observations in this paper are based on measurements made at Jakobshavn Isbræ (Figure 1) from May 2007 to August 2008. Data collection included several time-lapse cameras pointed at the glacier and fjord, optical and GPS surveys of glacier and iceberg motion, a pressure sensor for measuring ocean waves, a seismometer, and an audio recorder. All instruments recorded in UTC.

[8] Anywhere from one to six time-lapse cameras were pointed at the terminus and inner fjord between 13 May 2007 and 3 August 2008. The camera systems consisted of a variety of Canon digital cameras, Canon timers, and custom-built power supplies. Four of the cameras were used to capture the seasonal evolution of the glacier's terminus position, which varies ~5 km over the course of a year [*Joughin et al.*, 2008c; *Amundson et al.*, 2008]. The photo interval for these cameras ranged from 10 min to 6 h, depending on data storage capacity and the amount of time between field campaigns. The other two cameras took photos of the terminus every 10 s during two field campaigns (from $8-12$ May 2008 and from $9-25$ July 2008) to capture the full sequence of calving events; they captured nine events before failing. One additional camera was placed ~10 km down fjord from the terminus and pointed in the down fjord direction; it took photos every hour from 16 May to 9 July 2008 and every 15 min from 9 July to 6 August 2008. During our field campaigns all camera clocks were occasionally checked to correct for clock drift.

[9] Optical surveying prisms were deployed on the lower 4 km of the glacier in both 2007 (7 prisms) and 2008 (10 prisms). The prisms were surveyed with a Leica TM1800 automatic theodolite and DS3000I Distomat every $10-15$ min, weather permitting, from 15 May to 9 June 2007 and from 12 July to 4 August 2008. In 2007 five prisms lasted more than 18 days, three of which lasted the entire field campaign. In 2008 one prism lasted the entire field campaign and another lasted 17 days; all others fell over or calved into the ocean within nine days of deployment. The error in the surveyed positions was esti-
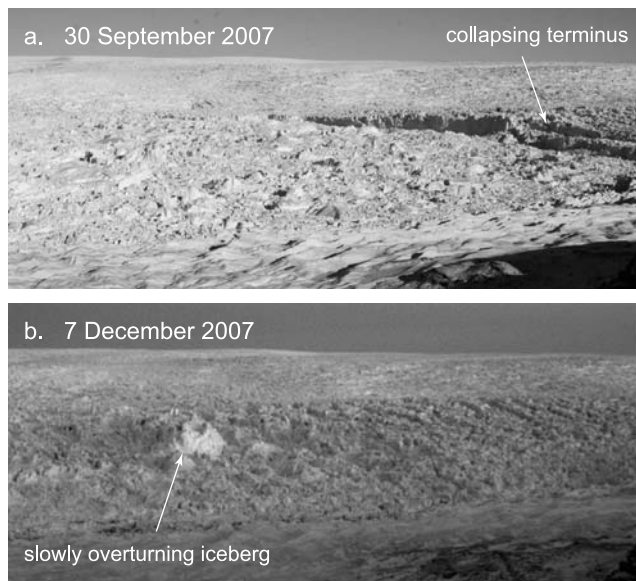
Figure 2. Time-lapse imagery of the ice mélange. (a) In late September 2007 the terminus began to collapse but was unable to push the mélange out of the way. The slump was present until a calving event on 17 October 2007. (b) A large iceberg in the mélange began overturning on 27 November 2007 and slowly rotated over the course of more than 3 weeks. Note the smooth transition between ice mélange and floating tongue.

mated to be ±0.15 m [*Amundson et al.*, 2008]. The position data were smoothed with a smoothing spline (using the curve fitting toolbox in MATLAB) and differentiated to calculate velocities. Errors in the velocity calculations are not easily estimated, though we can provide bounds over various time intervals: 0.21 m d^{-1} for daily average velocities, and 0.85 m d^{-1} for 6 h average velocities.

[10] Iceberg motion was measured with custom built L1-only GPS receivers that were designed for rapid deployment from a hovering helicopter. In 2007 we used a Vexcel microserver ("brick"; http://robfatland.net/seamonster/index.php?title=Vexcel_Microservers). The microserver was connected to a wireless transmitter, enabling data retrieval from camp. In 2008 we used a similar, custom-built 1 W receiver.

[11] GPS data from both years were broken into 15 min intervals and processed as static surveys against a base station at camp. During some periods, such as when the icebergs were moving quickly, we also processed the data using Natural Resources Canada's precise point positioning tool in kinematic mode. The positional uncertainty, determined by calculating the standard deviation of a detrended section of data, was typically around 1.0 m regardless of whether the data were processed as static or kinematic surveys. As with the optical surveying data (above), the position data were smoothed with a smoothing spline and differentiated to calculate velocities. Error bounds are 1.4 m d^{-1} for daily average velocities, and 5.7 m d^{-1} for 6 h average velocities.

[12] Ocean stage was measured every 5 s from 15–24 July 2008 with a Global Water water level sensor (model WL400) that recorded to a Campbell Scientific CR10X data logger. The sensor had a range of 18.3 m; its output was digitized to a resolution of 4×10^{-3} m. The instrument was placed in a small tide pool roughly 3 km from the glacier terminus; it was not rigidly attached to the ocean bottom but was weighted with ~5 kg of rocks.

[13] A Mark Products L22 three-component velocity seismometer was deployed on bedrock south of the terminus. The instrument has a natural frequency of 2 Hz and a sensitivity of 88 V s m^{-1}. The data were sampled with a Quanterra Q330 datalogger and baler. The sample frequency was 200 Hz from 17 May to 17 August 2007 and 10 May to 3 August 2008, and 100 Hz from 22 August 2007 to 9 May 2008.

[14] Audio signals were recorded in stereo with two Sennheiser ME-62 omnidirectional condenser microphones separated by 50 m; stereo recording enabled determination of the instrument to source direction. The microphones were powered by Sennheiser K6 power modules and connected to a Tascam HD-P2 stereo audio recorder with Audio Technica XLR microphone cables. The frequency response of the microphones ranges from 20 Hz to 20 kHz and is flat up to 5 kHz. Rycote softie windshields were used to reduce wind noise; they have virtually no effect on signals with frequencies higher than ~400 Hz but cause a 30 dB reduction in signals with frequencies lower than ~80 Hz. The recorder gain was set at 8 (out of 10); it logged with a sample frequency of 44.1 kHz and recorded WAV (waveform audio format) files to 8 GB compact flash cards. The flash cards were swapped every 12 h. The time was recorded when starting and stopping the 12 h sessions; we estimate that the instrument time was always within 2 s of UTC. Nearly continuous recordings were made from 8–14 May 2008 and 13 July to 2 August 2008.

3. Results

3.1. Temporal Variations in Terminus and Ice Mélange Dynamics

[15] The behavior of Jakobshavn Isbræ's ice mélange is highly seasonal and tightly linked to terminus dynamics. In winter, calving ceases, the terminus advances and develops a short floating tongue, and the mélange and newly formed sea ice are pushed down fjord as a cohesive unit at the speed of the advancing terminus [see also *Joughin et al.*, 2008c]. The mélange strengthens sufficiently to inhibit the overturning of unstable icebergs and furthermore, the floating tongue and ice mélange become nearly indistinguishable in time-lapse imagery (Figure 2). The terminus becomes clearly identifiable only after the floating tongue disintegrates in spring.

[16] Motion of the ice mélange is highly episodic in summer (Movie S1 of the auxiliary material) [see also *Birnie and Williams*, 1985; *Amundson et al.*, 2008].[1] Between calving events the mélange moves down fjord at roughly the speed of the advancing terminus (~40 m d^{-1}). One to two days prior to a calving event the mélange and lowest reaches of the glacier can accelerate up to ~60 m d^{-1} (Figures 3a–3b). This acceleration results in 10–20 m of additional displacement and could be due to
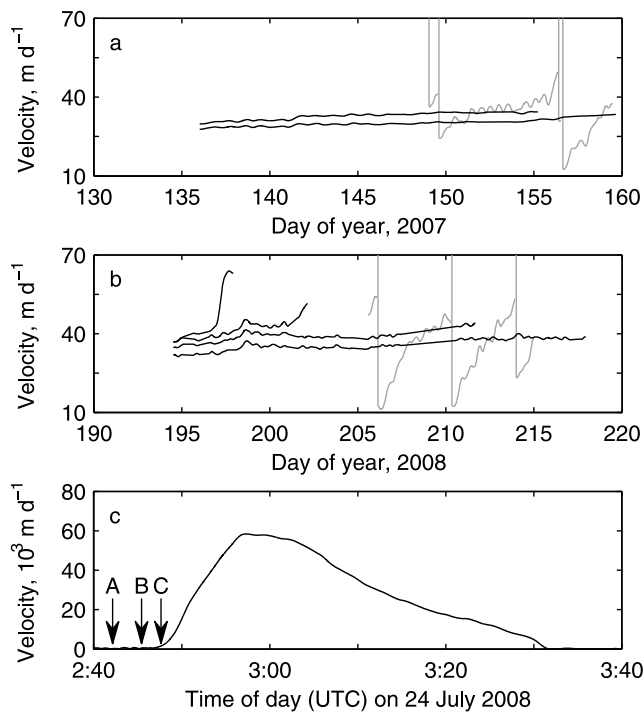

Figure 3. Measurements of iceberg and glacier motion. Velocity of an iceberg (gray) and of survey markers on the lower reaches of the glacier (black) during (a) summer 2007 and (b) summer 2008. The large jumps in iceberg velocity are coincident with calving events. The survey markers on the glacier accelerate as they approach the terminus and are eventually calved into the ocean. (c) Iceberg velocity during a calving event on 24 July 2008 (day of year 206; see Movie S4). Locations A, B, and C signify the onset of the calving-generated seismogram, the first evidence of activity in the fjord (a small iceberg close to the terminus collapsed), and the first sign of horizontal acceleration of the mélange away from the terminus, as seen in the time-lapse imagery.

rift expansion a short distance upglacier from the terminus. At the onset of a calving event the entire lateral width of the mélange rapidly accelerates away from the terminus, even if the event onset only involves a small portion of the terminus (Movies S2–S4). Rapid acceleration of the mélange away from the terminus does not appear to precede calving (Figure 3c). During a calving event the mélange can reach speeds greater than 50×10^3 m d^{-1} and extend longitudinally. Once calving ceases, frictional forces within the mélange and along the fjord walls cause the mélange to decelerate to roughly one half of the terminus velocity in $\sim$30 min. Over the next several days the mélange gradually reaccelerates until reaching the speed of the advancing terminus.

[17] In addition to the overall velocity variability described above, the mélange also experiences tidally modulated, semidiurnal variations in velocity with an amplitude of $\sim$4% of the background velocity. No vertical or horizontal tidal signals were observed on the glacier, indicating that the terminus is grounded in summer.

3.2. Glaciogenic Ocean Waves

[18] In addition to the rapid horizontal displacement of the ice mélange during calving events, ocean waves generated by calving icebergs cause the mélange to experience meters-scale vertical oscillations. Calving-generated waves can have amplitudes exceeding 1 m at a distance of $\sim$3 km from the terminus with dominant periods of 30–60 s (frequencies of 0.0017–0.033 Hz) (Figures 4a–4b; waves can also be seen in Movies S2–S4). Waves exceeding 1 m amplitude caused the pressure sensor, which was not rigidly attached to the seafloor, to move about in the water column. We are therefore unable to put a reliable upper bound on the size of the ocean waves. We note, though, that waves from one calving event tossed the sensor onto shore from a depth of 10 m. Furthermore, in the vicinity of the terminus, icebergs have been observed to experience vertical oscillations on the order of 10 m during calving events [Lüthi et al., 2009].

[19] Large calving events can also generate lower-frequency waves, with spectral peaks at 150 s and 1600 s (0.007 Hz and 6×10^{-4} Hz, respectively). These peaks likely represent eigenmodes (seiches) of the fjord; for example, the shallow water approximation predicts that the fundamental seiche period [e.g., Dean and Dalrymple, 1991] is 1250 s for a fjord that is $\sim$0.8 km deep [Holland et al., 2008; Amundson et al., 2008] and 55 km long. The long-period (1600 s) seiche generated on 19 July 2008 had
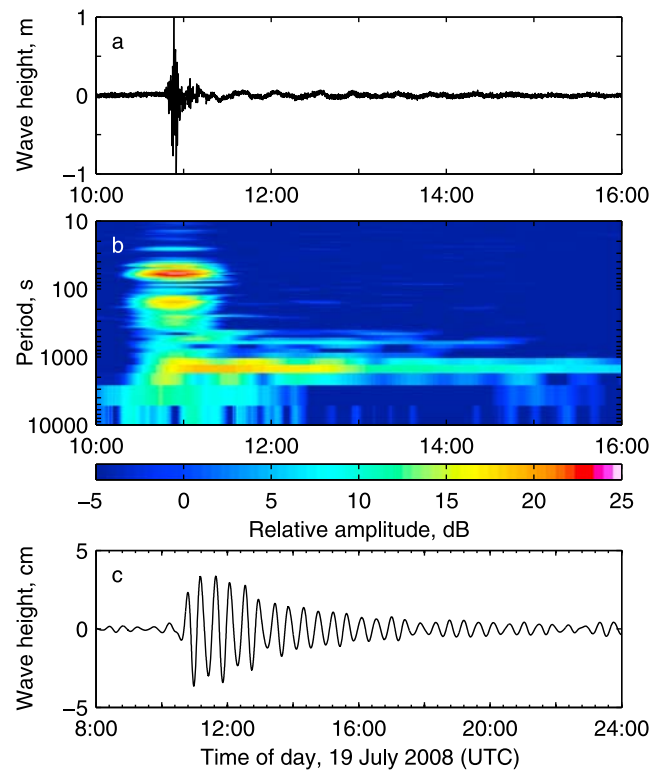

Figure 4. Ocean waves produced by a calving event on 19 July 2008. (a) Ocean stage during the calving event after filtering with a 7200 s high-pass filter to remove tidal signals. (b) Spectrogram of the ocean stage showing three spectral peaks. (c) 1000–2000 s band-pass filtered component of the wave; note the change in scale of the x and y axes.
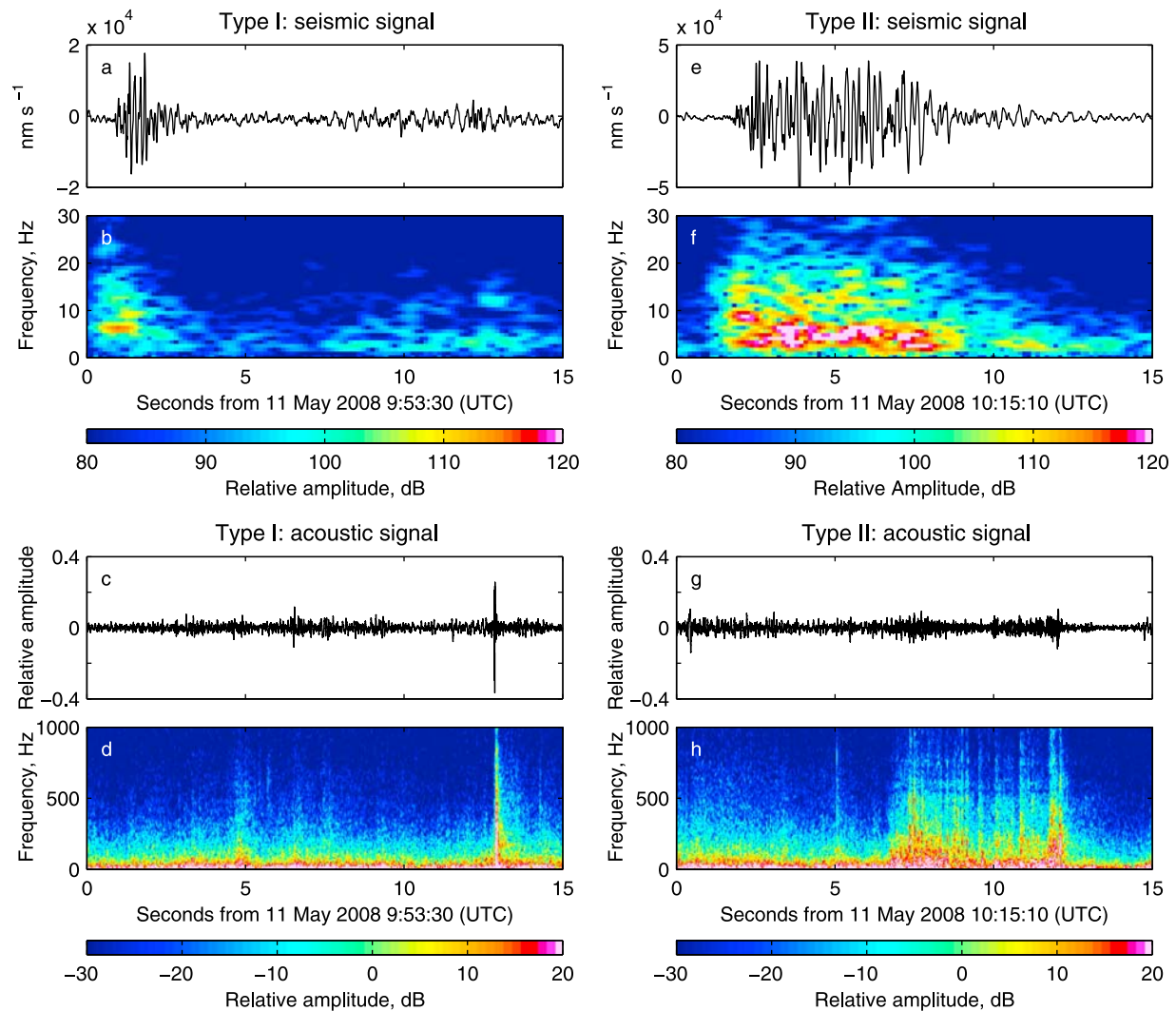
Figure 5. Examples of seismic signals originating in the fjord and terminus area. Type 1 (a−b) seismic signal and spectrogram and (c−d) associated acoustic signal. Type 2 (e−f) seismic signal and spectrogram and (g−h) associated acoustic signal.

a maximum amplitude of 0.035 m at the site of our pressure sensor, lasted over 8 h, and decayed with an e-folding time of roughly 3 h (Figure 4c). Given our limited observations, it is unclear whether these values are typical. Seiches from the calving events are also recorded in Ilulissat Harbor, over 50 km from the glacier terminus [*Amundson et al.*, 2008, Figure S2]; similar waves have been recorded at Helheim Glacier in east Greenland [*Nettles et al.*, 2008].

3.3. Seismic and Acoustic Signals Emanating From the Fjord

[20] Three main types of seismic signals were recorded by the seismometer: (1) impulsive signals with durations of 1−5 s and dominant frequencies of 6−9 Hz (Figures 5a–5b), (2) emergent signals with durations of 5−300 s and dominant frequencies of 4−6 Hz (Figures 5c−5d), and (3) long-lasting (5−60 min), emergent, high-amplitude signals generated by calving icebergs (Figure 6a) and by icebergs overturning during periods of quiescence at the terminus. The general characteristics of the type 3 signals

were discussed by *Amundson et al.* [2008]; we expand on those observations in section 4 with special attention paid to the event onsets and to the proportion of the seismograms that are attributable to motion of the ice mélange.

[21] The occurrence rate of type 1 and 2 signals (combined) was determined with a short-term averaging/long-term averaging (STA/LTA) detector after band-pass filtering the seismic data between 4 and 15 Hz. The STA/LTA ratio was computed using 0.2 s and 30 s windows, respectively, and events were triggered when the ratio exceeded 5. These values were chosen so as to detect both type 1 and 2 signals. Changing the detection parameters affected the total number of detections but did not affect the overall temporal variability. Type 1 and 2 signals can occur over 50 times per hour, with greatest activity during and immediately following calving events. On the hourly time scale, there is no obvious change in the number of events immediately preceding a calving event. Between calving events the occurrence rate can decay to less than 10 h^{-1}; the decay occurs with an e-folding time of roughly 12 h (Figure 7).
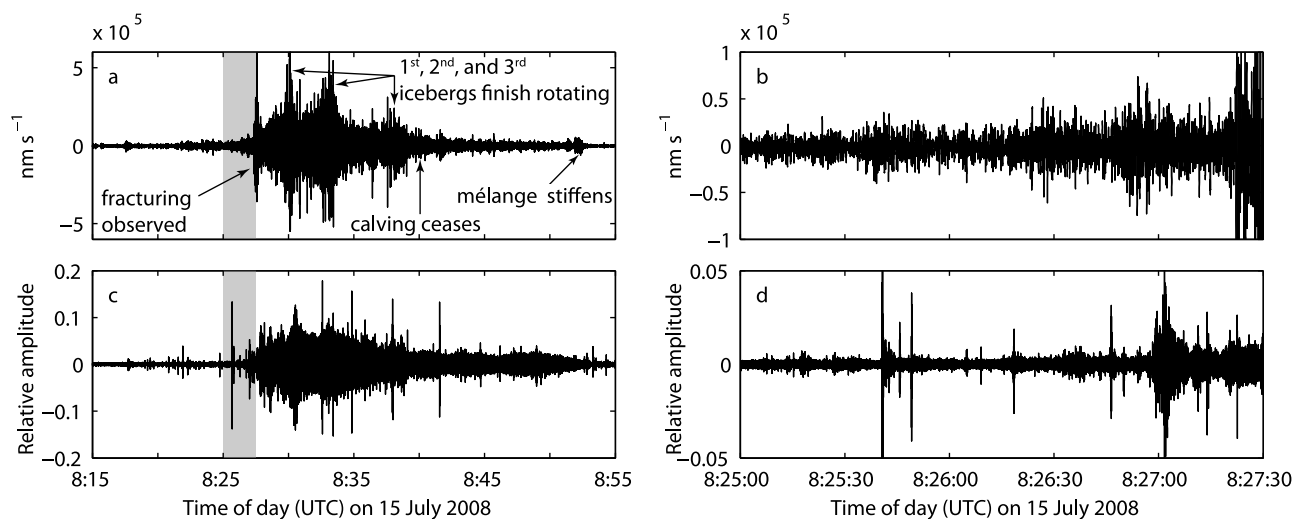
Figure 6. Seismic and acoustic waveforms from a calving event on 15 July 2008 (see also Movie S3). (a) Vertical component of the calving-generated seismogram. (b) A close-up of Figure 6a showing the emergent onset of the seismic signal. (c) Acoustic waveform from the calving event. (d) A close-up of Figure 6c. The gray bars in Figures 6a and 6c indicate the time periods shown in Figures 6b and 6d.

[22] When ambient acoustic noise levels (especially from wind) are low, many of the above-described seismic recordings are easily correlated with acoustic signals. Type 1 signals are associated with sharp cracking sounds ("shotgun blasts") suggestive of fracturing ice, whereas type 2 signals are associated with long, low rumblings indicative of avalanching ice debris. These acoustic signals contain significant energy at frequencies ranging from infrasonic (<20 Hz) to greater than 1 kHz (Figure 5). Stereo recordings of the acoustic signals indicate that they originate at the terminus and from down fjord at roughly equal rates. Calving-generated seismic signals (type 3) are associated with both cracking and rumbling sounds (Figures 6a and 6c).

4. Discussion of Calving Events

[23] The general characteristics of calving events and calving-generated seismograms at Jakobshavn Isbræ have been described by *Amundson et al.* [2008]. Here, we expand on those observations by comparing seismograms with audio recordings and high-rate time-lapse imagery that captures the onset of calving events. Event onsets are investigated in detail to determine whether calving events are triggered by motion of the mélange away from the terminus.

[24] The first sign of an impending calving event in the 10 s time-lapse imagery is generally either widespread fracturing (see spray of ice particles caused by seracs collapsing upglacier from the terminus in Movies S2 and S3) or avalanching of debris from the terminus (Movie S4). No previous motion could be detected by either feature tracking in oblique imagery or by differencing subsequent images. A small, gradual increase in seismic activity often precedes discernible motion of the terminus and ice mélange in the 10 s imagery (Figures 3c and 6a–6b and Movie S3, which shows the calving event discussed in Figure 6). The ramp-up in seismic activity coincides with an increase in the number of audible fractures and, to a lesser extent, debris avalanches, emanating from the fjord (see section 3.3;

Figure 6d). These sounds originate both at the terminus and in the fjord and are separated by periods of silence (i.e., there is no persistent background rumbling that is heard during calving events). We have so far been unable to detect any spatiotemporal patterns of acoustic signals preceding a calving event.

[25] The increases in seismic energy and number of acoustic signals in the short interval preceding discernible motion at the terminus also precede observed horizontal acceleration of the ice mélange (Figure 3c). Thus, motion of the mélange away from the terminus is not prerequisite for calving. The precursory activity in the fjord may instead represent unsettling of the mélange in response to a very small rotation of a large ice block at the glacier terminus. For example, rotating a 400 m long (in the glacier flow direction) by 1000 m tall iceberg by 0.5° will displace more than 4000 m^3 of water per meter of lateral width of the iceberg, yet the upper corner of the iceberg (point P_1 in Figure 8a) will move less than 0.02 m horizontally and 2 m vertically, while the point where the iceberg is in contact with the mélange (point P_2) will move 1 m horizontally. Such a small rotation at the terminus would therefore be undetectable with time-lapse photography or our on-iceberg GPS receivers, but may be sufficiently large to cause near-terminus icebergs to subtly shift their positions and thereby
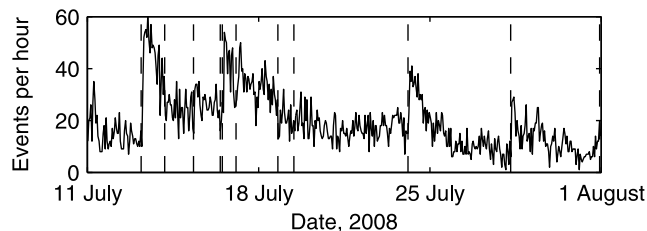

Figure 7. Temporal variations in the rates of short seismic events (type 1 and 2 combined). Calving events are indicated by dashed vertical lines.
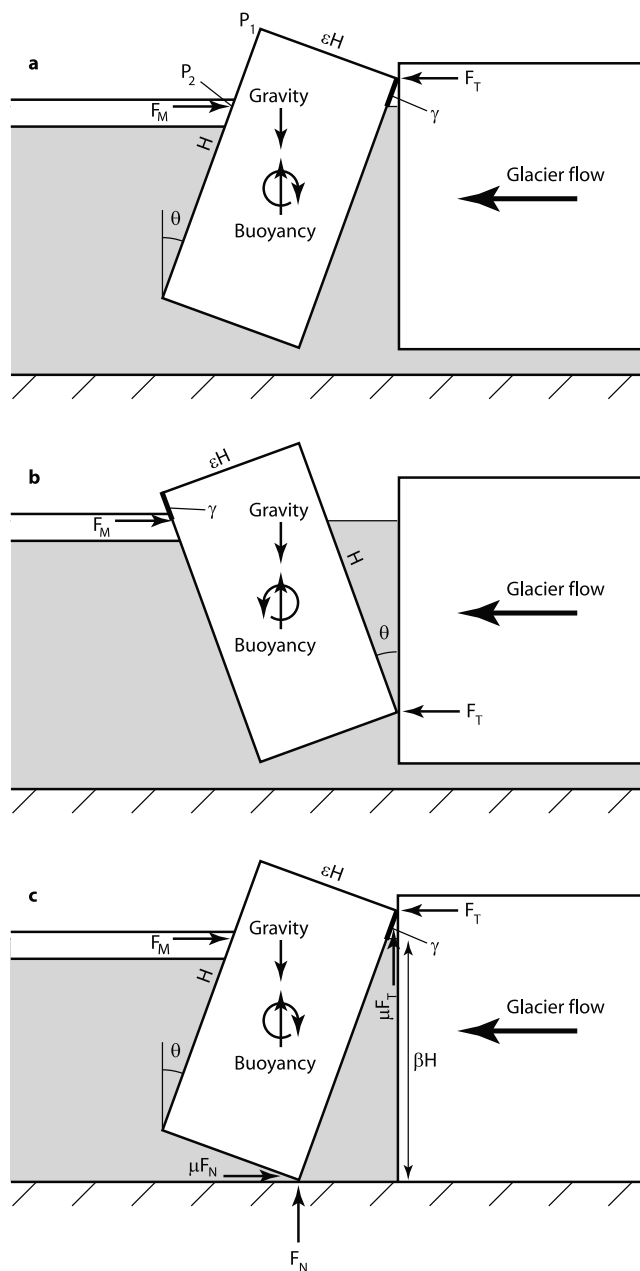
Figure 8. Diagrams used for the force balance analysis of calving icebergs. Here γ is indicated by thick black lines.

generate seismic and acoustic signals. We suggest that the emergent onsets of the seismograms represent the super-position of numerous fractures occurring at the terminus and in the mélange.

[26] Much of the seismic energy released during calving events at Jakobshavn Isbræ can, for several reasons, be attributed to horizontal and vertical motion of the ice mélange. First, maximum ground displacement coincides with the generation of large ocean waves, occuring imme-diately following the overturning of icebergs at the terminus (Movie S3 and Figure 6a). Second, ground displacement during the coda of the seismograms, which typically lasts 10 min or more, represents motion of the mélange only (i.e., the terminus is quiescent). The coda of the seismo-

gram therefore puts a minimum bound on the amount of ground displacement that can be generated through hori-zontal motion of the mélange. Third, there is a pronounced drop in seismic energy coincident with mélange stiffening as icebergs within the mélange have stopped overturning and the mélange has resumed steady deformation. Finally, the envelopes of the calving-generated seismic and acoustic waves have similar durations and several peaks that are temporally correlated, suggesting that the seismic and acous-tic waves have the same source. As discussed earlier, many of the acoustic signals emanate from the ice mélange.

[27] Calving-related seismograms are likely generated by a variety of mechanisms occurring simultaneously at numerous locations; they are therefore highly complex. Source mechanisms might include hydraulically driven frac-ture propagation and other hydraulic transients within the glacier [*St. Lawrence and Qamar*, 1979; *Métaxian et al.*, 2003; *O'Neel and Pfeffer*, 2007; *Winberry et al.*, 2009], the coalescence of microfractures at the terminus [*Bahr*, 1995], acceleration of the glacier terminus [*Nettles et al.*, 2008], ocean wave action [*Amundson et al.*, 2008; *MacAyeal et al.*, 2009], icebergs scraping the glacier terminus and fjord walls [*Amundson et al.*, 2008; *Tsai et al.*, 2008], and motion of an ice mélange or layer of sea ice. Superposition of these seismic signals makes interpretation of calving-generated seismograms exceedingly difficult. The interpretations can be improved with, among other things, simultaneous acoustic (including infrasonic and hydroacoustic) recordings. Glaciogenic acoustic signals are more impulsive and decay more rapidly than corresponding seismic signals (Figures 6b and 6d). Identifying and locating events may therefore be somewhat easier with acoustic recordings than with seismic recordings (see also J. Richardson, manuscript in preparation, 2009).

5. Simple Force Balance Analysis of Calving

[28] Motion of the ice mélange is clearly driven by terminus dynamics. The relationship is not, however, uni-directional. Here, we use a simple force balance analysis to argue that the mélange influences the seasonality of calving events and the sequence of individual calving events, includ-ing iceberg size and rotation direction. The force balance analysis also demonstrates that full-glacier-thickness ice-bergs, which dominate the glacier's mass loss from calving, are unable to calve from a well-grounded terminus.

[29] First, consider the case in which a rectangular iceberg of thickness H and width ϵH (perpendicular to the terminus) calves from a floating tongue (Figures 8a–8b). Rotation of the iceberg is driven by buoyant forces and, ignoring friction, inhibited by contact forces at the terminus, F_t, and the mélange, F_m. For simplicity, we assume that the force from the mélange can be treated as a horizontal line load acting at sea level, so that $|F_t| = |F_m|$.

[30] Summing the torques around the iceberg's center of mass for a block that is rotating bottom out (Figure 8a), we find that F_m required to hold the block in static equilibrium for some given tilt angle, θ, is

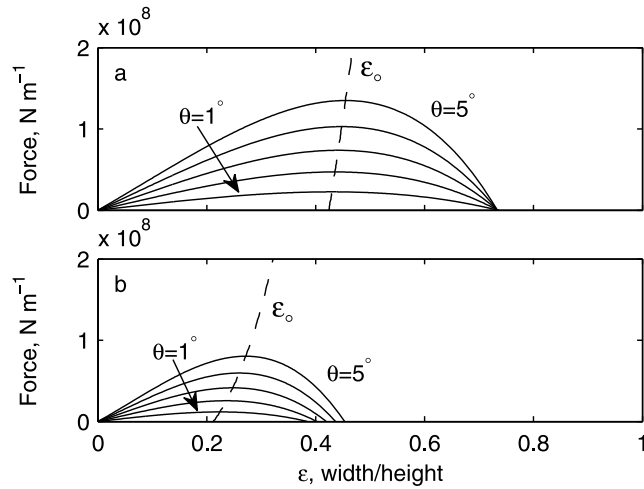$$F_m^b = \frac{-\sum_{i=1}^{3} \tau_i}{\gamma \cos \theta},$$ (1)

Figure 9. Force from the ice mélange (per meter lateral width) for various ϵ and θ that is required to decelerate an already overturning iceberg or to prevent an iceberg from overturning in the first place. These calculations assume that there is no friction at the contact points. Calving is considered from (a) a floating terminus and (b) a terminus that is at floatation ($\beta = \rho_i/\rho_w$). The dashed lines give the value of ϵ_o for various θ.

where superscript b denotes bottom out rotation, τ_i represents the torques from the water pressure acting along each of the iceberg's three submerged sides, $\gamma = H(1 - \rho_i/\rho_w - (\epsilon/2)\tan\theta)$ (see Figure 8 for the geometric interpretation of γ), and ρ_i and ρ_w are the densities of ice and water, respectively (adapted from *MacAyeal et al.* [2003]). If the force from the mélange is greater than the value given in equation (1), then the torques on the iceberg will either decelerate an iceberg's rotation or prevent an iceberg from rotating in the first place.

[31] Similarly, the force from the melange required to keep the block from rotating top out (Figure 8b) is

$$F_m^t = \frac{-\sum_{i=1}^{3}\tau_i}{H(\cos\theta - \epsilon\sin\theta) - \gamma\cos\theta}, \tag{2}$$

where superscript t denotes top out rotation. The ratio of these two forces is

$$\frac{F_m^b}{F_m^t} = \frac{\cos\theta - \epsilon\sin\theta}{(1 - \rho_i/\rho_w - (\epsilon/2)\tan\theta)\cos\theta} - 1. \tag{3}$$

In the limit that $\theta \to 0$, this ratio becomes

$$\frac{F_m^b}{F_m^t} = \frac{\rho_i}{\rho_w - \rho_i} \approx 9. \tag{4}$$

At small θ the force from the mélange required to keep a block from rotating bottom out is roughly 1 order of magnitude greater than the force required to keep a block from rotating top out. In other words, the resistive torque from a given F_m is greater for an ice block that is rotating top out

than it is for a block that is rotating bottom out. Thus, in the presence of a resistive ice mélange, bottom out rotation is strongly preferred over top out rotation. Without a mélange, there is no preferred direction of rotation in this simple, frictionless model.

[32] The force from the mélange (equation (1)) required to maintain static equilibrium is ultimately a function of H, ϵ, and θ. By arbitrarily setting $H = 1000$ m, approximately equal to the terminus thickness of Jakobshavn Isbræ, and using the equations for τ_i derived by *MacAyeal et al.* [2003], we can investigate the relationship between F_m^b and ϵ for various θ (Figure 9a).

[33] The maximum value of ϵ for which buoyant forces will cause an iceberg to overturn at arbitrarily small θ is $\epsilon_{cr} \approx 0.73$. Furthermore, the largest force required from the ice mélange to prevent rotation occurs when $\epsilon = \epsilon_o \approx 0.42$; icebergs of this geometry are therefore more easily able to capsize than thinner or wider icebergs. In this model, ϵ_o corresponds to the iceberg geometry that experiences the largest buoyancy-driven torque at small θ.

[34] If the terminus is instead grounded (Figure 8c, with $\mu = 0$), the force and torque balances give

$$F_m^b = \frac{-\sum_{i=1}^{3}\tau_i - H/2(F_g - F_b)(\epsilon\cos\theta - \sin\theta)}{H(\cos\theta - \beta)}. \tag{5}$$

where F_g and F_b are the gravitational and buoyant forces, $\beta = H_w/H$ and H_w is the water depth at the terminus, τ_i is the same as before, but γ (on which τ_i depends) is replaced with

$$\gamma = H(1 - \beta\sec\theta). \tag{6}$$

Here, when the terminus is just grounded (i.e., $\beta = \rho_i/\rho_w \approx 0.9$), $\epsilon_{cr} = 0.40$ and $\epsilon_o = 0.21$ for small θ (Figure 9). At certain water depths, a terminus may be floating but at such an elevation that calving icebergs will come into contact with the fjord bottom during overturning. In such cases, ϵ_{cr} and ϵ_o will be intermediate to the values given above.

[35] Including friction and/or lowering the water level below floatation further reduces ϵ_{cr}, ϵ_o, and the resistive force from the mélange required to prevent overturning. For example, ignoring the mélange (letting $F_m = 0$) but accounting for friction at the terminus and fjord bottom, the force and torque balances on the calving iceberg (Figure 8c) become

$$F_t - \mu F_n = 0, \tag{7}$$

$$\mu F_t + F_n = F_g - F_b, \tag{8}$$

$$\tau = \sum_{i=1}^{3}\tau_i + F_t H\left(\cos\theta + \frac{\mu}{2}(\sin\theta + \epsilon\cos\theta)\right) + F_n\frac{H}{2}(\epsilon\cos\theta - \sin\theta), \tag{9}$$

where F_n is the normal force on the fjord bottom, τ is the net torque acting on the iceberg, and μ is the coefficient of
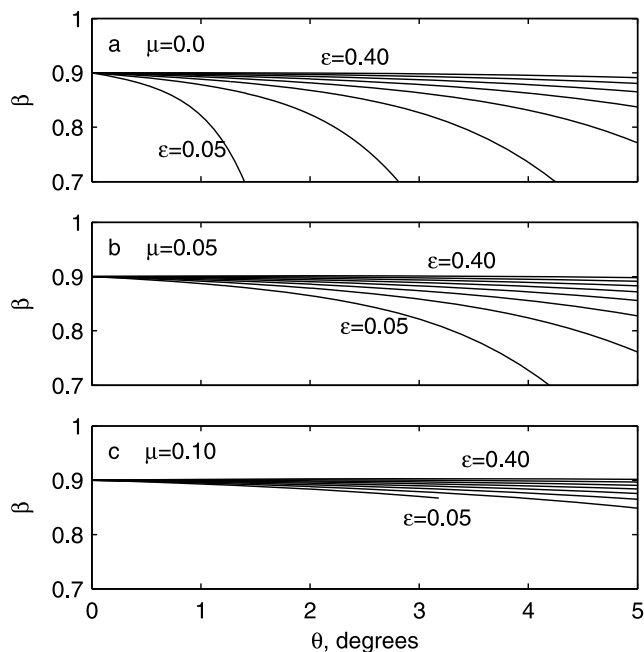
Figure 10. Minimum β (water depth divided by ice thickness) for which buoyant forces will cause a grounded iceberg with width ϵH and tilt from vertical θ to overturn. (a–c) Coefficients of friction, μ, between the iceberg and terminus and iceberg and fjord bottom were varied from $0-0.1$.

friction between the iceberg and the terminus and the iceberg and the fjord bottom (for simplicity, we assume that the coefficients of friction are the same for both points of contact). The curves in Figure 10 indicate the points at which $\tau = 0$ for various μ, ϵ, θ, and β. μ was varied from 0 to 0.1; these values are less than the coefficient of friction between ice and sand determined by sliding a relatively smooth, meter-scale ice block across a sand beach [*Barker and Timco*, 2003]. In order for buoyant forces to cause an iceberg of a given width-to-height ratio to overturn, the point in $\beta - \theta$ space must be above the appropriate $\tau = 0$ curve. From these curves it is apparent that buoyant forces are unable to cause the calving of realistically sized, full-glacier-thickness icebergs unless the water depth is close to or greater than $\frac{\rho_i}{\rho_w} H$ (Figure 10). A resistive ice mélange, not accounted for here, would further reduce the glacier's ability to calve from a grounded terminus, even if full-thickness fracture has occurred.

6. Interpretation

6.1. Mélange and Fjord Dynamics

[36] Motion of the ice mélange is driven by terminus dynamics. Between calving events the mélange is pushed down fjord by the advancing terminus [see also *Joughin et al.*, 2008c]. During these periods ocean and wind currents have little effect on mélange motion, at least within $15-20$ km of the glacier terminus (Movie S1). Previously, however, ephemeral turbid upwellings were observed at the terminus [*Echelmeyer and Harrison*, 1990], indicating that subglacial discharge occasionally caused local separation

between the mélange and terminus. We observed no such upwellings during $2007-2008$, thus suggesting that the recent increase in the glacier's calving flux has resulted in a denser, stronger mélange. Such changes may affect glacier dynamics (section 6.2), the timing and sequence of calving events (section 6.3), and damping of ocean waves [e.g., *Squire*, 2007, and references therein].

[37] As full-glacier-thickness icebergs calve and overturn, they rapidly push the ice mélange down fjord (Figure 3), sweep through ~ 0.5 km^3 of water as they rotate through $90°$, and may disrupt fjord stratification and circulation (as described in the work of *Motyka et al.* [2003]) by turbulently mixing the entire water column. The total volume of water affected by a single calving iceberg is likely larger than 0.5 km^3, since water must fill the void left by the calving iceberg at the same time that water is being pushed down fjord by the rotating iceberg. A typical calving event involves the calving of several full-glacier-thickness icebergs, which combined might displace more than 2 km^3 of water. Roughly thirty such calving events occur each year [*Amundson et al.*, 2008]. For comparison, the glacier's subglacial discharge, which drives fjord circulation, was estimated at $8-15$ km^{3}a^{-1} in the 1980s [*Echelmeyer et al.*, 1992]. Thus, calving events may strongly influence fjord circulation and affect the ability of deep, warm ocean water to reach the terminus. In a mélange-covered fjord, ocean currents may be further influenced by the irregular basal topography of the mélange.

[38] The currents and meters-scale ocean waves generated by calving events may help icebergs rotate to more energetically favorable positions (with larger width to height ratios), resulting in extension of the mélange [see also *MacAyeal et al.*, 2009]. Although the mélange is eventually recompacted by the advancing terminus (following calving events the mélange is initally moving slower than the terminus; Figures 3a and 3b), extension of the mélange during calving events may weaken it and reduce its ability to prevent subsequent calving events. Such weakening may explain, in part, why calving events occur more frequently in mid to late summer and nearly always involve the successive calving of several icebergs [*Amundson et al.*, 2008].

6.2. Mélange Influence on Glacier Dynamics

[39] The force required to prevent the calving and overturning of an iceberg at the glacier terminus (Figure 9) is comparable to the change in back force on the terminus due to tides. If the tidal range is 2 m and the mean water depth is 800 m, the range in back force, ΔF_p is

$$\Delta F_p = \frac{1}{2} \rho_w g \left(801^2 - 799^2 \right) \approx 1.6 \times 10^7 \text{N m}^{-1}. \quad (10)$$

[40] Tides appear to have little to no effect on the glacier's flow speed [see also *Amundson et al.*, 2008, Figure 1b], especially when compared to other tidewater glaciers such as Columbia Glacier, Alaska [*Walters and Dunlap*, 1987]. Thus, the mélange does not necessarily have a significant, direct influence on glacier velocity.

[41] On the other hand, our results show that the mélange can inhibit calving, thereby helping to enable terminus advance in winter. The floating tongue that currently develops in winter may be little more than an agglomeration

of ice blocks that are unable to overturn (such as the partially overturned iceberg in Figure 2b). Nonetheless, the newly formed floating tongue reduces the longitudinal strain rates at the grounding line, resulting in thickening and an associated increase in effective (ice overburden minus pore water) pressure there. Basal motion is generally thought to be highly sensitive to effective pressure, especially when the effective pressure is close to zero [e.g., *Paterson*, 1994, and references therein], as is likely the case near the termini of tidewater glaciers [*Pfeffer*, 2007]. Thus, a slight thickening near the grounding line in winter may be sufficient to explain the glacier's current seasonal velocity variations. Furthermore, the winter advance changes the geometry and stress distribution of the lower glacier; such changes have been shown to dramatically affect the glacier's flow, even without the inclusion of potential buttressing effects along the fjord walls (M. P. Lüthi, manuscript in preparation, 2009).

6.3. Sequence of Calving Events and Glacial Earthquakes

[42] Although the mélange may not directly influence glacier motion, it may affect the sequence of individual calving events. In section 5 we demonstrated that in the presence of a back force from the mélange, bottom out rotation of calving icebergs is strongly preferred over top out rotation and that icebergs with optimal width-to-height ratios ($\epsilon = \epsilon_o$) are more easily able to calve than icebergs of different dimensions. ϵ_o depends on the glacier's proximity to floatation and the coefficients of friction at points of contact with the terminus and fjord bottom, but is always less than 0.42 (Figure 9). Our observations indicate that ϵ for full-glacier-thickness icebergs that calve and overturn is generally between 0.2 and 0.5 (Movies S2–S4).

[43] The force balance analysis, which is consistent with our field observations, suggests that calving events begin with the bottom out rotation of icebergs with relatively small width-to-height ratios. Calving onset may be aided by avalanching of the terminus, which increases the buoyant torque on the newly formed iceberg, and/or by a subglacial outburst flood that rotates the iceberg away from the terminus [see also *O'Neel et al.*, 2007]. As the first iceberg calves, the mélange is pushed away from the terminus, both by the rotating iceberg and potentially by turbulent ocean currents generated by the rotating iceberg. Due to a reduction in back forces as the mélange accelerates away from the terminus, subsequent calving icebergs can more easily calve from a grounded terminus, rotate top out, and have larger width-to-height ratios. The latter two points are consistent with observations from the time-lapse imagery (see Movies S2 and S4). Furthermore, glacial earthquakes have recently been associated with calving events [*Joughin et al.*, 2008a; *Tsai et al.*, 2008; *Amundson et al.*, 2008; *Nettles et al.*, 2008] and hypothesized to be generated by especially large icebergs pushing off of the terminus [*Tsai et al.*, 2008] or scraping the fjord bottom [*Amundson et al.*, 2008]. If either of these glacial earthquake mechanisms is correct, then glacial earthquake generation should occur several minutes after calving onset, as has been observed [see *Amundson et al.*, 2008, Figure S4; *Nettles et al.*, 2008, Figure 3].

[44] The value of ϵ_o may affect the timing of calving events. For example, if a crevasse penetrates the entire glacier thickness at some distance $\epsilon_o H$ from the glacier terminus, the resulting iceberg may calve more readily than if the crevasse had penetrated the entire glacier thickness at a distance of $\epsilon H \neq \epsilon_o H$ from the terminus.

[45] Our analysis has mostly neglected the relationship between the mélange and the calving of tabular ($\epsilon \geq 1$) or nearly tabular ($\epsilon_{cr} \leq \epsilon \leq 1$) icebergs, which presently occurs during spring and winter when all or part of the terminus is floating and previously occurred year-round. Although our observations on the generation of tabular and near-tabular icebergs are limited, we have twice witnessed the calving of tabular icebergs at the end of long calving events (Movie S5) during the month of May. Both of these icebergs originated near the centerline of the glacier, where the terminus appeared to be partially ungrounded. Tabular icebergs might therefore only be able to detach from the glacier's terminus after previous, overturning icebergs have calved and pushed the mélange away from the glacier.

[46] Although the mélange may influence the timing and sequence of calving events, once a calving event begins and the mélange accelerates away from the terminus, the total mass loss during the event may be controlled by other factors and processes, such as preexisting fractures in the glacier [*Bahr*, 1995; *Benn et al.*, 2007, and references therein], the glacier's height above buoyancy [*Van der Veen*, 1996; *Vieli et al.*, 2001] (see section 6.4), and weakening of the terminus by large glaciogenic ocean waves [*MacAyeal et al.*, 2006, 2009]. The first point, that the total mass loss from a calving event is determined by the presence (or absence) of large rifts, is consistent with our visual observations. Thus, unless the back force exerted by the mélange is strong enough to influence rifting, in summer the total mass loss from calving over time scales of weeks to months is likely controlled by glacier dynamics and not by mélange strength. On annual or longer time scales, the total mass loss from calving may be influenced by the proportion of the year during which the mélange is strong enough to prevent calving events [*Joughin et al.*, 2008c]. Thus the mélange can affect the seasonality of the terminus position, which in turn affects the glacier's longer-term behavior.

6.4. Floatation Condition for Calving

[47] The calving of full-glacier-thickness icebergs is likely necessary to balance Jakobshavn Isbræ's high flow rates: between large calving events the terminus can easily advance more than 100 m despite the frequent calving of small (meter to several meter scale) icebergs. However, full-glacier-thickness icebergs are unable to capsize at small θ if the terminus is well grounded (Figure 10; section 5), even if full thickness fracture has occurred. Therefore a necessary, but not sufficient, condition for calving retreat is that the terminus is close to floatation. The ratio of water depth to ice thickness, β, necessary for calving depends on iceberg geometry and on the coefficients of friction at the iceberg's contact points; it is therefore difficult to assign a specific floatation condition for calving. However, for realistic iceberg geometries ($\epsilon = 0.25$) and a likely conservative coefficient of friction ($\mu = 0.05$), buoyancy-driven capsize will not occur unless $\beta > 0.875$ (Figure 10b).

[48] Due to buoyancy differences between ice and water, the immediate result of a full-thickness calving event from a grounded terminus is to increase the terminus' height above floatation (unless the glacier has a reverse bedrock

slope that is more than nine times the surface slope). Thus, although full-thickness calving events can be enabled by processes that change the torque balance on the terminus, such as avalanching of debris or subglacial discharge events, such processes cannot drive terminus retreat over long time periods.

[49] During its current retreat, Jakobshavn Isbræ's average rate of retreat was largest in the early 2000s [*Podlech and Weidick*, 2004; *Csatho et al.*, 2008] when the terminus was floating year-round. By 2004 the glacier had stopped producing tabular icebergs in summer (as can be seen in satellite imagery), suggesting that the glacier had evolved to calve grounded (or nearly grounded) ice in summer. At that time there was also a sharp decrease in the glacier's average rate of retreat [*Joughin et al.*, 2008c]. One potential explanation for this change is that the process limiting the glacier's rate of retreat switched from rift propagation in floating ice to dynamic thinning of grounded ice, processes occurring over different time scales. Thus, as long as the terminus region is sufficiently fractured, a height-above-floatation calving criterion (as proposed by *Van der Veen* [1996]) may give a reasonable assessment of the glacier's late summer terminus position. Such a criterion, which does not account for fracturing, is unable to predict individual calving events or to explain the growth and decay of a short floating tongue in winter [*Benn et al.*, 2007].

7. Conclusions

[50] Temporal variations in ice mélange strength can influence the evolution of Jakobshavn Isbræ's terminus position, and therefore glacier flow [*Nick et al.*, 2009; M. P. Lüthi, manuscript in preparation, 2009], by controlling the timing of calving events. Furthermore, motion of the ice mélange is strongly controlled by terminus dynamics, especially with respect to frequency and size of calving events.

[51] In winter, sea ice growth between icebergs (freezing of the mélange matrix) and at the mélange's seaward edge acts to stengthen the mélange, thus preventing calving and enabling the terminus to advance ~5 km. The mélange is pushed down fjord as a cohesive unit by the advancing terminus. The sea ice margin begins to retreat from the fjord mouth in midwinter; calving rejuvenates in spring after the sea ice margin has retreated to within a few kilometers of the glacier terminus. Once calving renews, motion of the mélange becomes highly episodic, especially during periods of frequent calving. Large, full-glacier-thickness calving events cause the mélange to rapidly move 2–4 km down fjord, extend longitudinally, and be subjected to vertical oscillations lasting over 12 h and having peak amplitudes greater than 1 m. This wave action may promote further disintegration of the terminus and ice mélange (as also suggested by *MacAyeal et al.* [2006, 2009]), resulting in additional seaward expansion and thinning of the mélange. Between calving events the mélange is recompressed and pushed forward by the advancing terminus, as occurs throughout winter.

[52] Our observations and simple force balance analysis demonstrate that the presence of a mélange influences calving behavior: the first iceberg to calve tends to be small and always rotates bottom out, whereas subsequent calving icebergs can be larger and rotate any direction. Motion of the mélange away from the terminus does not appear to be prerequisite for calving to begin. However, when the mélange is activated during calving onset, it loses the ability to resist the calving of subsequent icebergs. The total amount of ice lost during a calving event is therefore likely controlled by parameters other than mélange strength, such as the presence (or absence) of preexisting rifts upglacier. Thus it is unlikely that the ice mélange controls the net calving flux in summer over time periods of days to weeks. Over seasonal time scales or longer, the mélange could influence the net calving flux by controlling the proportion of the year during which calving can occur [*Joughin et al.*, 2008c]. Although the resistive force from the mélange may be insufficient to directly influence glacier motion, the mélange may indirectly influence glacier dynamics by controlling the evolution of the terminus geometry, which in turn affects glacier motion (M. P. Lüthi, manuscript in preparation, 2009). Finally, the calving behavior observed at Jakobshavn Isbræ is unable to occur when the glacier is well grounded (especially in the presence of a resistive ice mélange), suggesting that the net annual calving retreat is limited by the glacier's height above floatation.

[53] A realistic model of terminus behavior must be able to predict seasonal variations in calving rate. We suggest that at Jakobshavn Isbræ, these variations are presently controlled by variations in sea ice cover and ice mélange strength and by dynamic thinning of grounded ice in summer. The greater challenge is to couple the seasonality of ice mélange strength to the growth and decay of sea ice.

References

Abdalati, W., W. Krabill, E. Frederick, S. Manizade, C. Martin, J. Sonntag, R. Swift, R. Thomas, W. Wright, and J. Yungel (2001), Outlet glacier and margin elevation changes: Near-coastal thinning of the Greenland Ice Sheet, *J. Geophys. Res.*, *106*(D24), 33,729–33,741.

Amundson, J. M., M. Truffer, M. P. Lüthi, M. Fahnestock, M. West, and R. J. Motyka (2008), Glacier, fjord, and seismic response to recent large calving events, Jakobshavn Isbræ, Greenland, *Geophys. Res. Lett.*, *35*, L22501, doi:10.1029/2008GL035281.

Bahr, D. B. (1995), Simulating iceberg calving with a percolation model, *J. Geophys. Res.*, *100*(B4), 6225–6232.

Barker, A., and G. Timco (2003), The friction coefficient for a large ice block on a sand/gravel beach, paper presented at 12th Workshop on the Hydraulics of Ice Cover Rivers, CGU HS Comm. on River Ice Processes and the Environ., Edmonton, Alberta, Canada.

Benn, D. I., C. R. Warren, and R. H. Mottram (2007), Calving processes and the dynamics of calving glaciers, *Earth Sci. Rev.*, *82*, 143–179.

Birnie, R. V., and J. M. Williams (1985), Monitoring iceberg production using LANDSAT, in *Proceedings of the University of Dundee Summer School*, *Eur. Space Agency Spec. Publ.*, *SP-216*, 165–167.

Braun, M., A. Humbert, and A. Moll (2009), Changes of Wilkins Ice Shelf over the past 15 years and inferences on its stability, *Cryosphere*, *3*, 41–56.

Copland, L., D. R. Mueller, and L. Weir (2007), Rapid loss of the Ayles Ice Shelf, Ellesmere Island, Canada, *Geophys. Res. Lett.*, *34*, L21501, doi:10.1029/2007GL031809.

Csatho, B., T. Schenk, C. J. Van der Veen, and W. B. Krabill (2008), Intermittent thinning of Jakobshavn Isbræ, west Greenland, since the Little Ice Age, *J. Glaciol.*, *54*(184), 131–144.

Dean, R. G., and R. A. Dalrymple (1991), *Water Wave Mechanics for Engineers and Scientists*, 353 pp., World Sci., Singapore.

Echelmeyer, K., and W. D. Harrison (1990), Jakobshavns Isbræ, west Greenland: Seasonal variations in velocity — or lack thereof, *J. Glaciol.*, *36*(122), 82–88.

Echelmeyer, K., W. D. Harrison, T. S. Clarke, and C. Benson (1992), Surficial glaciology of Jakobshavns Isbræ, west Greenland: Part II. Ablation, accumulation and temperature, *J. Glaciol.*, *38*(128), 169–181.

Geirsdóttir, Á., G. H. Miller, N. J. Wattrus, H. Björnsson, and K. Thors (2008), Stabilization of glaciers terminating in closed water bodies: Evidence and broader implications, *Geophys. Res. Lett.*, *35*, L17502, doi:10.1029/2008GL034432.

Higgins, A. K. (1991), North Greenland glacier velocities and calf ice production, *Polarforschung*, *60*(1), 1–23.

Holland, D. M., R. H. Thomas, B. DeYoung, M. H. Ribergaard, and B. Lyberth (2008), Acceleration of Jakobshavn Isbræ triggered by warm subsurface ocean waters, *Nat. Geosci.*, *1*, 659–664, doi:10.1038/ngeo316.

Howat, I. M., I. Joughin, S. Tulaczyk, and S. Gogineni (2005), Rapid retreat and acceleration of Helheim Glacier, east Greenland, *Geophys. Res. Lett.*, *32*, L22502, doi:10.1029/2005GL024737.

Howat, I. M., I. Joughin, M. Fahnestock, B. E. Smith, and T. A. Scambos (2008), Synchronous retreat and acceleration of southeast Greenland outlet glaciers 2000–06: Ice dynamics and coupling to climate, *J. Glaciol.*, *54*(187), 646–660.

Joughin, I., W. Abdalati, and M. Fahnestock (2004), Large fluctuations in speed on Greenland's Jakobshavn Isbræ glacier, *Nature*, *432*, 608–610.

Joughin, I., I. Howat, R. B. Alley, G. Ekstrom, M. Fahnestock, T. Moon, M. Nettles, M. Truffer, and V. C. Tsai (2008a), Ice-front variation and tidewater behavior on Helheim and Kangerdlugssuaq Glaciers, Greenland, *J. Geophys. Res.*, *113*, F01004, doi:10.1029/2007JF000837.

Joughin, I., S. B. Das, M. A. King, B. E. Smith, I. M. Howat, and T. Moon (2008b), Seasonal speedup along the western flank of the Greenland Ice Sheet, *Science*, *320*, doi:10.1126/science.1153288.

Joughin, I., I. M. Howat, M. Fahnestock, B. Smith, W. Krabill, R. B. Alley, H. Stern, and M. Truffer (2008c), Continued evolution of Jakobshavn Isbræ following its rapid speedup, *J. Geophys. Res.*, *113*, F04006, doi:10.1029/2008JF001023.

Krabill, W., et al. (2004), Greenland Ice Sheet: Increased coastal thinning, *Geophys. Res. Lett.*, *31*, L24402, doi:10.1029/2004GL021533.

Luckman, A., T. Murray, R. de Lange, and E. Hanna (2006), Rapid and synchronous ice-dynamic changes in east Greenland, *Geophys. Res. Lett.*, *33*, L03503, doi:10.1029/2005GL025428.

Lüthi, M. P., M. Fahnestock, and M. Truffer (2009), Calving icebergs indicate a thick layer of temperate ice at the base of Jakobshavn Isbræ, Greenland, *J. Glaciol.*, *55*(191), 563–566.

MacAyeal, D. R., T. A. Scambos, C. L. Hulbe, and M. A. Fahnestock (2003), Catastrophic ice-shelf break-up by an ice-shelf-fragment-capsize mechanism, *J. Glaciol.*, *49*(164), 22–36.

MacAyeal, D. R., et al. (2006), Transoceanic wave propagation links iceberg calving margins of Antarctica with storms in tropics and Northern Hemisphere, *33*, L17502, doi:10.1029/2006GL027235.

MacAyeal, D. R., E. A. Okal, R. C. Aster, and J. N. Bassis (2009), Seismic observations of glaciogenic ocean waves (micro-tsunamis) on icebergs and ice shelves, *J. Glaciol.*, *55*(190), 193–206.

Métaxian, J.-P., S. Araujo, M. Mora, and P. Lesage (2003), Seismicity related to the glacier of Cotopaxi Volcano, Ecuador, *Geophys. Res. Lett.*, *30*(9), 1483, doi:10.1029/2002GL016773.

Moon, T., and I. Joughin (2008), Changes in ice front position on Greenland's outlet glaciers from 1992–2007, *J. Geophys. Res.*, *113*, F02022, doi:10.1029/2007JF000927.

Motyka, R. J., L. Hunter, K. A. Echelmeyer, and C. Connor (2003), Submarine melting at the terminus of a temperate tidewater glacier, LeConte Glacer, Alaska, U.S.A., *Ann. Glaciol.*, *36*, 57–65.

Nettles, M., et al. (2008), Step-wise changes in glacier flow speed coincide with calving and glacial earthquakes at Helheim Glacier, Greenland, *Geophys. Res. Lett.*, *35*, L24503, doi:10.1029/2008GL036127.

Nick, F. M., A. Vieli, I. M. Howat, and I. Joughin (2009), Large-scale changes in Greenland outlet glacier dynamics triggered at the terminus, *Nat. Geosci.*, *2*, 110–114, doi:10.1038/NGEO394.

O'Neel, S., and W. T. Pfeffer (2007), Source mechanics for monochromatic icequakes produced during iceberg calving at Columbia Glacier, AK, *Geophys. Res. Lett.*, *34*, L22502, doi:10.1029/2007GL031370.

O'Neel, S., H. P. Marshall, D. E. McNamara, and W. T. Pfeffer (2007), Seismic detection and analysis of icequakes at Columbia Glacier, Alaska, *J. Geophys. Res.*, *112*, F03S23, doi:10.1029/2006JF000595.

Paterson, W. S. B. (1994), *The Physics of Glaciers*, 3rd ed., 481 pp., Butterworth-Heinemann, Oxford, U. K.

Pfeffer, W. T. (2007), A simple mechanism for irreversible tidewater glacier retreat, *J. Geophys. Res.*, *112*, F03S25, doi:10.1029/2006JF000590.

Podlech, S., and A. Weidick (2004), A catastrophic break-up of the front of Jakobshavn Isbræ, west Greenland, 2002/2003, *J. Glaciol.*, *50*(168), 153–154.

Reeh, N., H. H. Thomsen, A. K. Higgins, and A. Weidick (2001), Sea ice and the stability of north and northeast Greenland floating glaciers, *Ann. Glaciol.*, *33*, 474–480.

Rignot, E., and P. Kanagaratnam (2006), Changes in the velocity structure of the Greenland Ice Sheet, *Science*, *311*, 986–990, doi:10.1126/science.1121381.

Scambos, T., H. A. Fricker, C.-C. Liu, J. Bohlander, J. Fastook, A. Sargent, R. Massom, and A.-M. Wu (2009), Ice shelf disintegration by plate bending and hydro-fractures: Satellite observations and model results of the 2008 Wilkins ice shelf break-ups, *Earth Planet. Sci. Lett.*, *280*, 51–60.

Sohn, H.-G., K. C. Jezek, and C. J. van der Veen (1998), Jakobshavn Glacier, west Greenland: 30 years of spaceborne observations, *Geophys. Res. Lett.*, *25*(14), 2699–2702.

Squire, V. A. (2007), Of ocean waves and sea-ice revisited, *Cold Reg. Sci. Technol.*, *49*, 110–133.

St. Lawrence, W., and A. Qamar (1979), Hydraulic transients: A seismic source in volcanoes and glaciers, *Science*, *203*, 654–656.

Thomas, R. H. (1979), Ice shelves: A review, *J. Glaciol.*, *24*(90), 273–286.

Thomas, R. H., W. Abdalati, T. L. Akins, B. M. Csatho, E. B. Frederick, S. P. Gogineni, W. B. Krabill, S. S. Manizade, and E. J. Rignot (2000), Substantial thinning of a major east Greenland outlet glacier, *Geophys. Res. Lett.*, *27*(9), 1291–1294.

Tsai, V. C., J. R. Rice, and M. Fahnestock (2008), Possible mechanisms for glacial earthquakes, *J. Geophys. Res.*, *113*, F03014, doi:10.1029/2007JF000944.

Van der Veen, C. J. (1996), Tidewater calving, *J. Glaciol.*, *42*(141), 375–385.

Vieli, A., M. Funk, and H. Blatter (2001), Flow dynamics of tidewater glaciers: A numerical modelling approach, *J. Glaciol.*, *47*(59), 595–606.

Walters, R. A., and W. W. Dunlap (1987), Analysis of time series of glacier speed: Columbia Glacier, Alaska, *J. Geophys. Res.*, *92*(B9), 8969–8975.

Winberry, J. P., S. Anandakrishnan, and R. B. Alley (2009), Seismic observations of transient subglacial water-flow beneath MacAyeal Ice Stream, west Antarctica, *Geophys. Res. Lett.*, *36*, L11502, doi:10.1029/2009GL037730.

_____

J. M. Amundson, R. J. Motyka, and M. Truffer, Geophysical Institute, University of Alaska Fairbanks, 903 Koyukuk Dr., Fairbanks, AK 99775-7320, USA. (amundson@gi.alaska.edu)

J. Brown and M. P. Lüthi, Versuchsanstalt für Wasserbau, Hydrologie und Glaziologie, ETH Zürich, Gloriastrasse 37–39, CH-8092 Zürich, Switzerland.

M. Fahnestock, Institute for the Study of the Earth, Oceans and Space, University of New Hampshire, 39 College Rd., Durham, NH 03824, USA.